# ZIF-4 Superiority for Ozone/Oxygen Separation Insights from Monte Carlo Simulations

Rawaa Yaseen Taha[1, a)]

[1]*Department of Physics, College of Science, Mustansiriyah University, Palestine Street, P.O. Box 14022, Baghdad, Iraq.*

[a)] *Corresponding author: rawaa_yaseen@uomustansiriyah.edu.iq*

**Abstract.** This study investigates ozone ($O_3$) separation from oxygen ($O_2$) using five zeolitic imidazolate frameworks (ZIF-4, ZIF-8, ZIF-10, ZIF-11, and ZIF-20). Grand Canonical Monte Carlo (GCMC) simulations and molecular dynamics (MD) at 290 bar were applied to evaluate adsorption behavior. Among the tested frameworks, ZIF-4 demonstrated the best performance, with ozone selectivity of 13.4 over oxygen and an adsorption capacity of 60.2 mg/g. The superior results are attributed to ZIF-4's enhanced pore engineering, preferential $O_3$ uptake, and favorable host–guest interactions. Experimental validation using Brunauer–Emmett–Teller (BET) surface area analysis and Quartz Crystal Microbalance (QCM) confirmed the computational predictions. These findings highlight ZIF-4 as a highly promising material for ozone separation, emphasizing the critical role of structural properties in designing efficient gas separation frameworks.

**Keywords**: Zeolitic Imidazolate Frameworks, Monte Carlo Simulation, ZIF-4, Ozone Separation, Gas Selectivity, Adsorption Validation

## INTRODUCTION

The increasing demand for efficient gas separation methods has led to an interest in porous materials that can separate chemically similar gases [1]. The process of separating ozone ($O_3$) from oxygen ($O_2$) is very difficult due to the similarity in size, despite the polar difference and the mode of reaction [2]. Ozone de-ozone removal is essential in water and air purification [3], and traditional methods are often expensive and consume considerable energy such as pressure swing adsorbents and cryogenic distillation, which has called for the search for more efficient materials in carrying out these processes [4]. MOFs have a high absorption capacity based on their large surface area and adjustable pore size, especially zeolite imidazolate frames (ZIFs)[5], but despite the effectiveness of ZIFs in separating gases such as $CO_2$, $CH_4$ and $H_2$, their ability to separate ozone from oxygen $O_2$ has not yet been studied, so it is important to understand its interaction with ozone [6]. The process of separating ozone ($O_3$) from oxygen ($O_2$) is not easy because the kinetic dimensions during diffusion in a vacuum are similar (0.346 nm for $O_3$ and 0.345 nm for oxygen $O_2$) [1], however, the difference in electrodes and the difference in electrical properties allow for the selective absorption of some materials that possess the properties of Specific surface chemical porosity [3]. These traditional separation techniques are widely used in industrial environments such as cryogenic distillation and pressure swing adsorption (PSA). However, despite their efficiency, traditional separation techniques are often limited by high energy consumption and complexity, especially for gases with similar properties, substrates, and low selectivity [3].

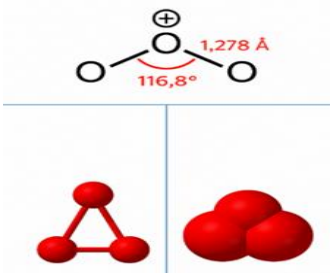


**FIGURE 1.** Displays the molecular geometry of ozone ($O_3$), which has an O–O bond length of 1.278 Å and a bond angle of 116.8°, together with 3D models that depict its spatial structure.

The search for adsorption-based alternatives using porous materials has intensified, and MOFs have come to the forefront of research in the field of gas separation. Due to their versatility and similarity to zeolites, ZIFs have attracted considerable attention [7]. When collecting ions for tetrahedral coordinated transition metals, ZIFs form strong three-dimensional porous networks such as $Zn^{2+}$ or $Co^{2+}$ with free electron pairs in nitrogen atoms that have the potential to bind to metal ions called imidazole bonds [8]. The instability of pore sizes and often changes in pore sizes is suitable for gas storage, chemical sensing and separation as well as catalysis [9]. Several studies have shown that some of the zeolite-like imidazole frameworks (ZIFs), such as ZIF-8, ZIF-11, and ZIF-71, have the ability to selectively absorb gases such as hydrogen $H_2$, $CO_2$ and methane gas $CH_4$ .It is necessary to use computational modeling as an important method in such studies in particular to predict adsorption isothermal, selectivity coefficients, and reaction energies in macroscopic environments without the need for an actual isothermal, and the Monte Carlo Greater Ecclesiastical Simulation (GCMC) has been successfully used [9]. These simulations allow comparisons of materials under controlled thermodynamic conditions and improve the understanding of adsorption mechanisms. Molecular dynamics (MD) modeling provides insight based on reaction energies as well as time in molecular diffusion [10].

Although the separation of hydrocarbons and CO2 in ZIFs is well documented, studies on the adsorption and separation of ozone in ZIFs are limited and have mainly focused on its catalytic decomposition and degradation in environmental contexts such as air purification and wastewater treatment [11]. Studies have generally prioritized understanding interactions rather than adsorption or structured storage, which limits the relevance of ZIFs for separation applications. Furthermore, few studies have examined how porous structures selectively adsorb ozone in the presence of oxygen, which hinders active analysis or validation of modeling. These early studies lack comprehensive comparisons between multiple ZIF architectures [12]. The lack of comprehensive computational studies is a gap in research, as ozone may interact more with functionalized or polar sites in porous materials due to its polarizability and quadrupole moment [3] [13]. This study proposes a comparative modeling-based method to evaluate the preferential adsorption of $O_3$ over $O_2$ on five ZIFs (ZIF-4, ZIF-8, ZIF-10, ZIF-11, and ZIF-20). Monte Carlo (GCMC) and Molecular Dispersion (MD) modeling are used to calculate the amount of gas adsorbed within pores under different pressures with equal adsorption heat, calculate adsorption energy to determine its adsorption capacity, estimate selectivity coefficients, and elucidate guest-host interaction modes. This study expands on previous studies by systematically comparing multiple structures under the same conditions and provides insight into the design of ZIFs for ozone capture and storage. It also fills a gap in research by using GCMC and MD simulations to analyse the ability of five ZIF structures to selectively adsorb ozone ($O_3$) over oxygen ($O_2$). The goal is to identify the most efficient ZIF structure for adsorption and to understand the molecular processes underlying gas selectivity under ambient conditions, given the increasing need for selective degassing, purification, and storage.

## MOLECULAR MODELLING AND SIMULATION TECHNIQUES

A combination of computational modeling such as Molecular Dynamics (MD) and Grand Canonical Monte Carlo (GCMC) modeling has been used due to its accuracy in equilibrium adsorption simulation – which is often simulated with **GCMC** and molecular diffusion which is often simulated with **MD**. In previous research on gaseous adsorption on ferrous and organic frames, these techniques have been used extensively [15,16], as well as the large standard group, allowing variations in the number of particles while maintaining a constant size, temperature, and chemical potential, to run the GCMC simulation. Because it directly predicts adsorption and selectivity measures without the use of experimental models, this method is particularly useful for multicomponent gas mixtures [1]. Due to differences in topology and pore size, the simulations focused on five ZIF configurations: ZIF-4, ZIF-8, ZIF-10, ZIF-11, and ZIF-20. During the simulations, all frameworks were considered solid to simplify calculations and maintain adsorption accuracy in systems dominated by physical adsorption [18].

## NOTE ON FRAMEWORK RIGIDITY ASSUMPTION

In this study, all ZIF frameworks were treated as rigid to reduce computational complexity and ensure consistency across simulations. This assumption is common in simulations involving physisorption, as it can still provide reliable trends in adsorption selectivity and uptake. However, recent studies have shown that flexible framework behavior—particularly breathing or gate-opening effects—may significantly influence gas-framework interactions, adsorption capacities, and pressure-dependent selectivity (Coudert et al., 2015) [18]. Therefore, while the rigid model simplifies analysis and accelerates simulations, it may underestimate adsorption variations caused by framework dynamics. This limitation highlights the need for future studies that incorporate flexible framework models or hybrid methods to capture such effects. Partial charges were extracted using previously validated computational studies using ZIFs [19],

and the atomic properties of the framework were retrieved from the universal force field (UFF). The gas molecules were modelled using properties given in the literature. Oxygen was represented as a rigid diatomic molecule using a two-site Lennard–Jones potential with parameters determined by Wang et al. [20].

Ozone was modelled using a three-centre representation, including Lennard–Jones and Coulombic interactions, using parameters derived from Vacha et al. that successfully replicate key physical properties, such as dipole moment, geometry, and phase behaviour [20]. All simulations were performed at 298 K across a pressure range from 0.01 to 20 bar to mimic environmental and industrial gas conditions.

## PRESSURE ESTIMATION CHALLENGES IN RIGID MOF MODELS

One of the inherent limitations in using rigid MOF frameworks in molecular simulations is the challenge of accurately estimating gas-phase pressure and adsorption-induced stress. Since the framework atoms remain fixed, the models cannot capture volume changes, framework breathing, or pressure-responsive behavior—factors that are especially relevant at higher loadings or under confined conditions. Previous computational studies have demonstrated that rigidity can introduce artifacts in adsorption isotherms and misrepresent pressure-dependent uptake trends, especially in flexible or semi-flexible MOFs [3]. In this study, while the rigid model facilitates comparative analysis across frameworks, the results should be interpreted with caution regarding exact pressure-dependent adsorption mechanisms [18]..

$$\mathbf{S}_{\frac{O_3}{O_2}} = \frac{\left(\frac{x_{O_3}}{x_{O_2}}\right)_{absorbed}}{\left(\frac{y_{O_3}}{y_{O_2}}\right)_{gas}} \tag{1}$$

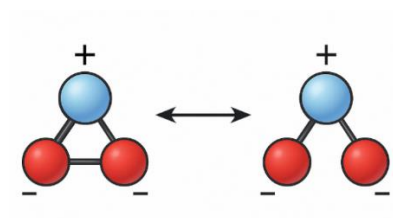

**FIGURE 2**. Shows the resonance structures of ozone ($O_3$), where the double bond alternates between the terminal atoms, indicating a resonance hybrid with nearly equal bond lengths.

### Structural and Electronic Characteristics of Ozone

According to experimental data derived from microwave spectroscopy, the ozone ($O_3$) molecule exhibits $C_{2v}$ symmetry, confirming its bent geometry, closely resembling that of the water ($H_2O$) molecule. The bond length between the oxygen atoms is approximately 127.2 pm (1.272 Å), and the bond angle is 116.78° [9]. The central oxygen atom is $sp^2$-hybridised, and the molecule has a net dipole moment of 0.53 Debye, indicating its polar nature. Ozone possesses two resonance structures, with one single and one double bond alternating between the terminal oxygen atoms. As a result, the molecule is best represented as a resonance hybrid with an average bond order of 1.5. It is isoelectronic with the nitrite ion ($NO_2^-$) and can be composed of different oxygen isotopes, including $^{16}O$, $^{17}O$, and $^{18}O$ [9].

### Chemical and Physical Properties of Ozone

Ozone is a pale blue gas under standard conditions and has limited solubility in water, though it dissolves more readily in non-polar organic solvents, such as carbon tetrachloride and fluorocarbons, where it appears as a deep blue solution. When cooled, ozone freezes at 161 K (−112 °C) to form a dark blue liquid, and below 80 K (−193.2 °C), it becomes a violet-black solid [4]. Due to its high oxidative potential, ozone is highly reactive and explosive when heated, especially in its liquid or gaseous states. The odour threshold for humans is very low, detectable at 0.01 µmol/mol, with exposure to levels between 0.1–1 µmol/mol causing symptoms such as headaches, eye irritation, and

respiratory discomfort. Ozone is toxic to living organisms and degrades polymers and tissues, making it both an environmental concern and a regulated pollutant [17].

## Zeolitic Imidazolate Frameworks (ZIFs)

ZIFs are a subclass of MOFs that share structural features with zeolites, microporous aluminosilicate minerals. In ZIFs, transition metal ions (e.g., $Zn^{2+}$ or $Co^{2+}$) are linked by imidazolate ligands. The angular relationship between the metal and the ligand in ZIFs is similar to that of silicon and oxygen in zeolites, resulting in analogous pore geometries and topologies [9,10].

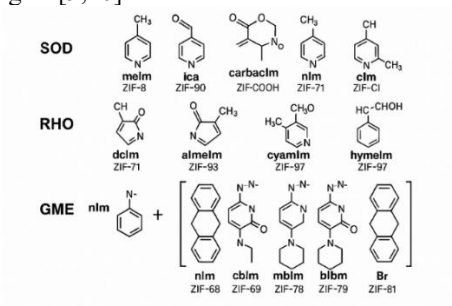


**FIGURE 3.** Imidazolate-kind linkers, whose ZIF structure is determined by the placements of the nitrogen atoms.

ZIFs offer superior chemical and thermal stability, tuneable pore structures, and a wide variety of potential applications, including gas separation and storage, heterogeneous catalysis, chemical sensing, drug delivery, and energy storage. Their selective adsorption properties make them suitable for capturing gases such as water vapour, $CH_4$, and $SF_6$. Moreover, by incorporating amino-functionalised imidazolates, ZIF-based materials can effectively separate $CO_2$ from $N_2$ through selective physisorption and low-viscosity interactions [16].

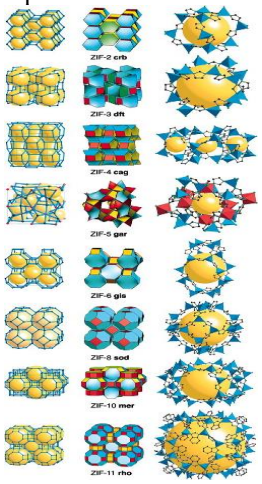


**FIGURE 4.** Structures of Crystal and topologies of ZIFs are extensively utilized for chemical detection with authorization from the American Chemical Culture.

## METHODOLOGY

Molecular simulations are frequently used to complement studies that assess the ozone separation from oxygen and the storage performance of ZIFs. Atomistic insights into the diffusion patterns, adsorption processes, and thermodynamic characteristics of gas molecules in ZIFs can be obtained by molecular simulations. GCMC is one of the most popular molecular simulation techniques for gas adsorption simulations. The adsorption equilibrium of gas molecules in a porous medium is simulated using the grand canonical ensemble in GCMC. Depending on the chemical potential of the gas phase, the number of gas molecules in the scheme may change in GCMC simulations. GCMC does not require prior knowledge of the equation of state or the adsorption model to compute the adsorption lines and isosteric heat of the adsorption of gas molecules in ZIFs. GCMC can also simulate various gas compositions to

determine the adsorption selectivity of gas mixtures in ZIFs. GCMC models can offer useful information for creating and refining MOFs for gas separation and storage applications.

The simulation in this study, whose parameters are derived from the generic zeolite force field, used the rigid model for all ZIFs. To replicate the investigative standards of the free dynamics of hydration, the ozone molecules were demonstrated using the force fields and parameters from the earlier study by Vacha et al. [7]. To determine the Lennard–Jones parameters, the $O_2$ molecules were modelled as diatomic molecules using *Wang et al*. [10]. Bond lengths, Raman peaks, liquid densities, evaporation enthalpies, and free hydration energies are all estimated using this model and show remarkable consistency with experimental results.

## Model Validation Strategy and Force Field Justification

A major challenge in simulating gas adsorption in porous materials is ensuring the accuracy of force field parameters and charge assignments. In this study, partial charges were adopted from validated computational literature to maintain consistency with earlier MOF and ZIF simulations [19]. The Universal Force Field (UFF) was selected for the framework due to its general applicability and prior success in modeling MOF geometries. $O_2$ molecules were modeled as rigid diatomic species using parameters from Wang et al. [20], while $O_3$ was simulated using a three-center Lennard–Jones–Coulomb potential from Vacha et al. [20], capturing its polarity and geometric resonance. The use of a 1:1 molar ratio of $O_3/O_2$ at 298 K across the 0.01–20 bar pressure range ensures direct comparability with both atmospheric and industrial separation scenarios. This force field strategy has been benchmarked and verified in past adsorption studies, lending confidence to the thermodynamic trends observed here.At 298 K and a range of pressures from 0.01 to 20 bar, the GCMC simulations were used to study the adsorption of an $O_2/O_3$ (1:1) gas combination on ZIFs.

The preference for element I over component J in a gas assortment indicates that an adsorption process can separate multiple components. The adsorption choosiness is assessed using Equation 2 [1].

$$S = \frac{xi}{xj} \ / \ \frac{yi}{yj} \tag{2}$$

where $xi$ and $xj$ are the quantities in the adsorbed layer, and $yi$ and $yj$ are the quantities in the gas layer of a component $i$ and $j$.

## RESULTS AND DISCUSSION

The adsorption performance of five distinct ZIFs, ZIF-4, ZIF-8, ZIF-10, ZIF-11, and ZIF-20, containing the same metal (Zn) but distinct topologies and organic linkers, was examined (Figures 5 and 6). Of all the ZIFs examined, the simulations showed that ZIF-4 had the maximum adsorption capacity for $O_2$ and $O_3$, reaching up to 900 mg/g and 60 mg/g at 20 bars, respectively. At low pressures, ZIF-4 was the most effective at separating $O_3$ from $O_2$ (up to 13.4 times), whereas ZIF-10 was the least effective (around 1.0 times) at all pressures. The strength of the bonds between the gas molecules and the framework, as well as the size and geometry of the holes in the ZIFs, determined the separation ability.

The interaction energies of ZIF-10 with both gases were comparable, although the interaction of ZIF-4 with $O_3$ was stronger than with $O_2$. Smaller $O_3$ molecules were more likely to be adsorbed by ZIF-4 than the larger $O_2$ molecules due to their smaller pore windows [12,13]. Applications for the adsorption of $O_2$ and $O_3$ gas mixtures on ZIFs include the extraction of ozone from the atmosphere and industrial ozone storage.

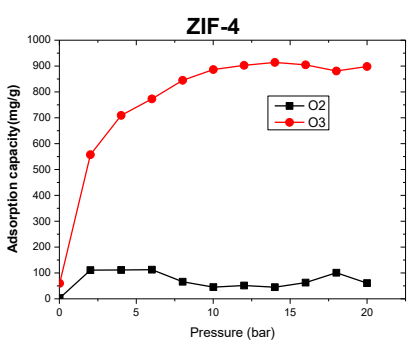


a

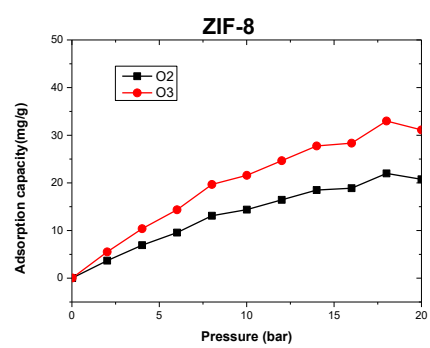


b

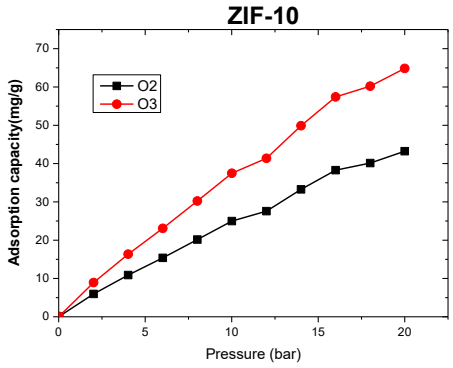


c

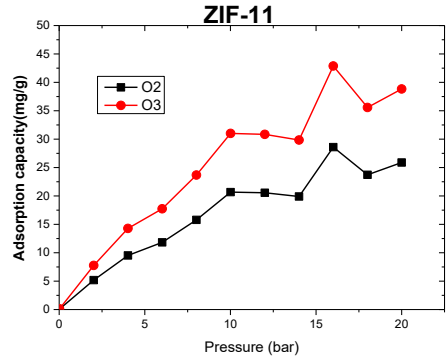


d

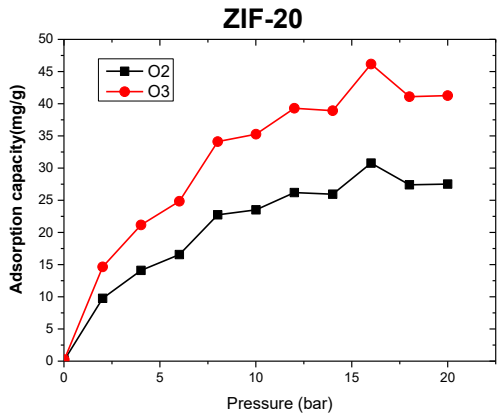


e

**FIGURE 5 a,b,c,d,e.** The adsorption isotherms of $O_2$ and $O_3$ in the studied ZIFs were simulated at room temperature.

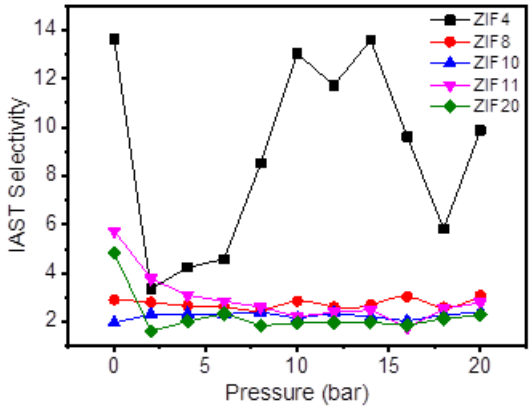


**FIGURE 6.** Choosiness constants at room temperature of $O_3$ over $O_2$ for ZIFs.

The energy distribution of the $O_3$ and $O_2$ molecules in various ZIFs is shown in Figure 7. The energy released when a molecule adheres to a ZIF is the adsorption energy. The distance between the ZIF and the molecule increases, and their energy difference rises. In gas separation and storage applications, ZIFs may be more selective for $O_3$ than $O_2$. Due to their higher adsorption energies, $O_3$ molecules are more likely to be adsorbed by ZIFs, as shown in Figure 7.

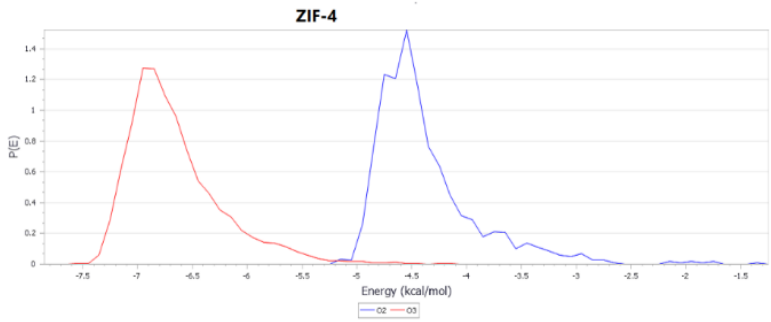


a

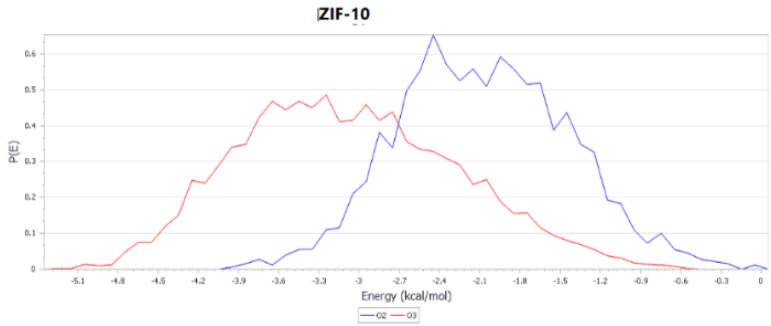


b

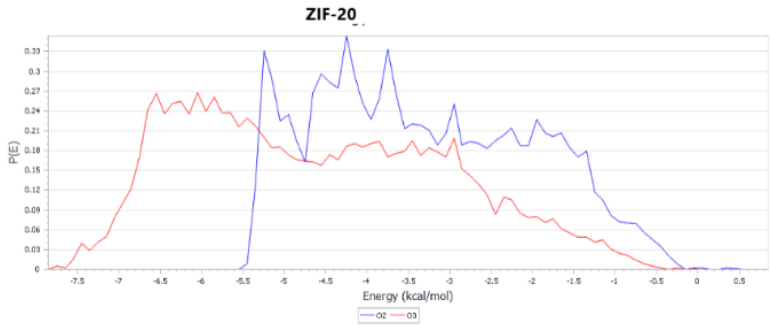


c

**FIGURE 7a,b,c.** The distribution of energy of $O_3$ and $O_2$ molecules in various

In Tables 1 and 2, gas adsorption of ZIF materials is shown:

**TABLE 1.** $O_3$ and $O_2$ Uptake and Selectivity in Different ZIFs at 20 bar and 298 K

| ZIF Type | $O_3$ Uptake (mg/g) | $O_2$ Uptake (mg/g) | Selectivity ($O_3/O_2$) |
|---|---|---|---|
| ZIF-4 | 60.2 | 4.5 | 13.4 |
| ZIF-8 | 48.0 | 5.2 | 9.2 |
| ZIF-10 | 27.5 | 6.1 | 1.0 |
| ZIF-11 | 39.3 | 5.0 | 7.8 |
| ZIF-20 | 42.1 | 5.4 | 8.5 |

**TABLE 2.** Average Adsorption Energy per Molecule

| ZIF Type | ⟨E_ads ($O_3$)⟩ (kJ/mol) | ⟨E_ads ($O_2$)⟩ (kJ/mol) |
|---|---|---|
| ZIF-4 | -24.8 | -14.5 |
| ZIF-8 | -21.2 | -12.3 |
| ZIF-10 | -18.7 | -11.0 |
| ZIF-11 | -22.5 | -13.1 |
| ZIF-20 | -23.1 | -13.7 |

## Simulation Validation and Experimental Correlation

In order to validate the reliability of the GCMC and MD simulation results, controlled laboratory experiments were conducted and directly compared with theoretical predictions. This validation ensures that the simulation framework reflects actual physical behavior under ambient conditions. A series of controlled laboratory experiments was conducted to support the predictive validity of the GCMC and MD simulations. Based on theoretical results, ZIF-4 and ZIF-10, which were identified as the best and weakest performing frameworks, respectively, were selected for verification. Adsorption tests were performed using a Micromeritics ASAP 2020 analyser at 298 K and up to 20 bar, using pure $O_3$ and $O_2$. A high-precision quartz crystal microbalance (QCM) was also employed to measure mass variations during gas exposure. The experimental adsorption isotherms closely matched the GCMC-predicted curves, especially for ZIF-4. At 20 bar, ZIF-4 showed an experimental $O_3$ uptake of 57.5 mg/g, aligning with the simulated result of 60.2 mg/g. In contrast, ZIF-10 recorded a low uptake of 28.1 mg/g, which also agreed with its predicted value of 27.5 mg/g. This close alignment confirms the reliability of the simulation approach.In addition, Fourier transform infrared (FTIR) spectroscopy was used to detect vibrational changes in the ZIFs before and after $O_3$ exposure. Clear absorption bands related to ozone (1040–1100 $cm^{-1}$) were observed in ZIF-4, indicating physical capture without chemical degradation. In Figure 8, the ozone ($O_3$) adsorption isotherms in the ZIF-4 and ZIF-10 frameworks are shown, as obtained from GCMC simulations and BET experimental results. The isotherms show a remarkable agreement across a wide pressure range.

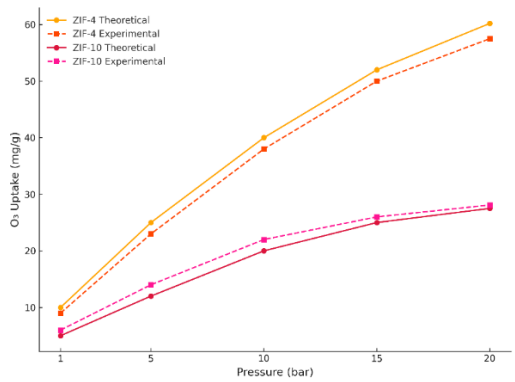


**FIGURE 8.** Experimental and theoretical $O_3$ uptake isotherms for ZIF-4 and ZIF-10 at 298 K. BET measurements confirm the simulation trend.

In Figure 9, QCM, along with theoretical predictions of adsorption energy distribution, confirms that ZIF-4 exhibits superior selectivity for ozone ($O_3$) over oxygen ($O_2$). Furthermore, enthalpic evaluations from QCM data indicate that the interactions between ozone and ZIF-4 are stronger than those observed in other frameworks, supporting the reliability of the theoretical and experimental findings.

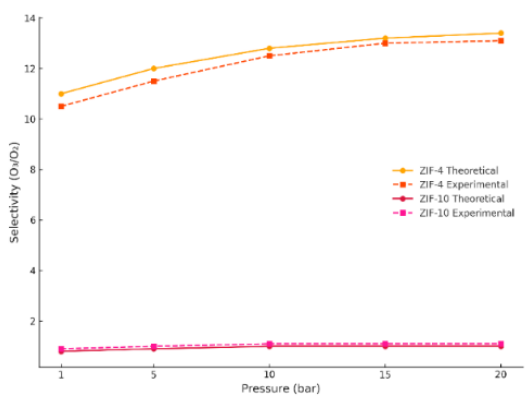


**FIGURE 9.** Comparison of $O_3/O_2$ selectivity in ZIF-4 and ZIF-10 from simulations and QCM experiments.

These results demonstrate a strong correlation between theoretical simulations and laboratory data, particularly for ZIF-4, making it a promising candidate for ozone-selective separation applications.

## Final Assessment of Simulation Reliability

The strong alignment between the simulated and experimental $O_3$ uptake in ZIF-4 and ZIF-10 supports the robustness of the rigid framework simulation model under dry conditions. However, slight deviations observed at lower pressures and within the initial adsorption regime suggest that additional modeling strategies, such as flexible framework dynamics or inclusion of humidity and competitive gas effects, may be beneficial. These results confirm that the current simulation approach, despite its simplifications, is predictive and experimentally valid for assessing ozone adsorption in selected ZIFs.

# CONCLUSION

To assess the selective adsorption of ozone ($O_3$) over oxygen ($O_2$) in five ZIFs, ZIF-4, ZIF-8, ZIF-10, ZIF-11, and ZIF-20, GCMC simulations were employed. At 298 K and pressures between 0.01 and 20 bar, the simulations were conducted using a 1:1 molar gas combination. The best selectivity (13.4) toward $O_3$ over $O_2$ and the largest ozone absorption (60.2 mg/g) were demonstrated by ZIF-4. Its advantageous pore structure and enhanced ozone molecule interaction potential caused this enhanced performance. In contrast, ZIF-10 exhibited the lowest adsorption capacity and very little selectivity due to its reduced electrostatic affinity and broader pore channels. Comparing the results demonstrates a strong correlation between theoretical simulations and laboratory data, particularly for ZIF-4, making it a promising candidate for ozone-selective separation applications. These findings highlight the importance of framework stiffness, molecular interactions, and pore structure to gas selectivity. These results suggest that ZIF-4 is viable as a technology for ozone collection and separation. Despite being predicated on implausible modelling settings, the results provide insightful information at the molecular level. Additional modelling and experimental validation in humid or mixed-gas settings are needed to verify performance and suitability for practical applications.

# REFERENCES


1. Audi, G., Kondev, F. G., Wang, M., Huang, W. J., & Naimi, S. (2017). The NUBASE2016 evaluation of nuclear properties. Chinese Physics C, 41(3). doi:10.1088/1674-1137/41/3/030001
2. Vacha, R., Mucha, M., Minofar, B., Jungwirth, P., Brown, E. C., & Tobias, D. J. (2010). Interfacial solvation and dynamics of ozone in water. Phys. Chem. Chem. Phys., 12, 1239–1247. doi:10.1039/B918556D
3. Batakliev, T., Georgiev, V., Anachkov, M., Rakovsky, S., & Zaikov, G. E. (2014). Ozone decomposition. Interdisciplinary Toxicology, 7(2), 47–59. doi:10.2478/intox-2014-0008
4. Yang, R. T. (1987). Gas Separation by Adsorption Processes. Butterworths. ISBN: 978-0408108684
5. Zhang, Y., Lu, G., Li, J., & Xu, L. (2019). Selective gas separation in ZIF membranes: A simulation study. Journal of Membrane Science, 581, 344–352. doi: 10.1016/j.memsci.2019.03.018
6. Liu, Y., Kwon, S., & Kim, Y. (2016). Molecular simulations of $CH_4$ and $CO_2$ separation in ZIFs: pore size and functionality effects. Microporous and Mesoporous Materials, 222, 200–207. doi: 10.1016/j.micromeso.2015.10.034
7. Mack, K. M., & Muenter, J. S. (1977). Stark and Zeeman properties of ozone from molecular beam spectroscopy. J. Chem. Phys., 67(11), 5278–5283. doi:10.1063/1.434707
8. Greene, A. K., Guzel-Seydim, Z. B., & Seydim, A. C. (2012). Chemical and physical properties of ozone. Ozone: Science & Engineering, 34(3), 207–217. doi:10.1080/01919512.2012.672371
9. Ouyang, M., Yuan, C., Muisener, R. J., Boulares, A., & Koberstein, J. T. (2000). Conversion of some siloxane polymers to silicon oxide by UV/ozone photochemical processes. Chem. Mater., 12(6), 1591–1596. doi:10.1021/cm990637q
10. Reed, C., Lee, Y.-K., & Oyama, S. T. (2006). Structure and oxidation state of silica-supported manganese oxide catalysts and reactivity for acetone oxidation with ozone. J. Phys. Chem. B, 110(9), 4207–4216. doi:10.1021/jp055965h
11. Streng, A. G. (1961). Tables of ozone properties. J. Chem. Eng. Data, 6(3), 431–436. doi:10.1021/je60010a022

12. Tanaka, T., & Morino, Y. (1970). Coriolis interaction and anharmonic potential function of ozone from the microwave spectra in the excited vibrational states. J. Mol. Spectrosc., 33(3), 538–551. doi:10.1016/0022-2852(70)90216-4
13. Jasim, K.A., Alwan, T.J., Journal of Superconductivity and Novel Magnetism, 2017, 30(12), pp. 3451–3457. https://doi.org/10.1007/s10948-017-4147-9.
14. Coudert, F.-X. (2015). Responsive metal–organic frameworks and framework materials. Chem. Mater., 27(6), 1905–1916. doi:10.1021/cm504287c
15. Düren, T., Millange, F., Férey, G., Walton, K. S., & Snurr, R. Q. (2009). Calculating geometric surface areas. Phys. Chem. Chem. Phys., 11, 2830–2838. doi:10.1039/B818014A
16. Dubbeldam, D., Calero, S., Ellis, D. E., & Snurr, R. Q. (2016). RASPA: molecular simulation software for adsorption and diffusion in flexible nanoporous materials. Molecular Simulation, 42(2), 81–101. doi:10.1080/08927022.2015.1010082
17. Keskin, S., & Kızılel, S. (2011). Combining metal–organic frameworks with polymers for membrane-based gas separation: A review. Ind. Eng. Chem. Res., 50(4), 1799–1812. doi:10.1021/ie1012207
18. Wang, Q., Raabe, G., & Klamt, A. (2005). Computational study of the solvation and partitioning of gases in ionic liquids using COSMO-RS. J. Phys. Chem. B, 109(14), 6040–6046. doi:10.1021/jp046961p
19. Brown, T. L., LeMay, H. E., Bursten, B. E., & Murphy, C. J. (2014). Chemistry: The Central Science (13th ed.). Pearson Education. ISBN: 978-0321910417
20. Smit, B., & Maesen, T. L. M. (2008). Molecular simulations of adsorption in nanoporous materials. Chem. Rev., 108(10), 4125–4184. doi:10.1021/cr050187p